PHYSICAL REVIEW B VOLUME 43, NUMBER 9 15 MARCH 1991-II

Inelastic scattering from surfaces

J. R. Manson
*Max-Planck-Institut für Strömungsforschung, Bunsenstrasse 10, D-3400 Göttingen, Federal Republic of Germany and Department of Physics and Astronomy, Clemson University, Clemson, South Carolina 29634**
(Received 18 October 1990)

A treatment of inelastic scattering of low-energy probes from surfaces is developed that bridges the gap between the zero- and single-quantum regime and the multiquantum regime. Observations of the multiphonon background directly give the form factor of the unit cell, which in turn provides information on the interaction potential. A semiclassical limit is extracted in which the differential reflected intensity appears as the product of a form factor for scattering from a unit cell, a Debye-Waller factor, a structure factor, and an energy exchange factor. This is compared with previously developed semiclassical scattering approximations. Good agreement is obtained with recently measured multiphonon backgrounds in the scattering of He by alkali halide and metal surfaces over a large range of surface temperatures and incident conditions. The comparisons with experiment demonstrate the rather large difference in interaction potentials between He scattering from an alkali halide and a metal surface.

I. INTRODUCTION

Inelastic stattering from surfaces provides important information on the bonding forces between surface atoms[1] and the nature of the surface electronic distribution.[2] There are several primary scattering probes which give surface-sensitive information, x-rays,[3] electrons,[4] and small-mass atoms.[5] This paper is primarily concerned with atomic probes, and in particular, we address the question of how much surface-specific information can be obtained without explicit knowledge of the interaction potential between probe and surface. Because many of the conclusions do not depend on the interaction potential, with suitable modification the methods and results can also be applied to other surface probes.

We briefly review elastic scattering and single-phonon inelastic scattering, but the major emphasis and new results are on exchanges of multiple-phonon quanta in the collision process. In principle, measurements of single-phonon scattering intensities directly provide the vibrational spectral densities of the surface atoms, which in turn depend on the surface bonding forces. However, the specific information on the phonon spectral density can be extracted only if the influence of the interaction potential is understood, since the intensity depends on both the spectral density and the scattering amplitude from the surface unit cell. An additional complication arises in the case of a surface unit cell with a basis, as, for example, a stepped or reconstructed surface. In this case the inelastic-scattered intensity is a much more complicated superposition of pairwise atomic spectral densities together with scattering amplitudes from all of the components of the unit cell. We show here that the multiphonon-scattering intensity can provide information on the interaction potential (or scattering amplitudes) which allows one to extract the spectral density from the single-phonon intensity measurements. Furthermore, for the more complicated case of unit cells with a basis, the multiphonon intensities provide information which can be useful in untangling the complicated dependence on the scattering potential, and can lead to information on the vibrational properties of individual components of the unit cell.

In a typical experiment with energy resolution of the scattered beam through time-of-flight methods, the elastic and single-surface-phonon intensities appear as sharp peaks, while the multiphonon contribution is usually assumed to provide a smooth and continuous background. However, recent studies[6] have demonstrated that in many circumstances the multiphonon background can have sharp features which, if not properly identified as such, could be mistaken as anomalous single-phonon peaks.

We consider here the multiphonon-background intensity of a quantum-mechanical theory, and at the end extract the semiclassical results which have been obtained previously,[7–10] and relate them to other numerical treatments.[11–13] We find, in agreement with the semiclassical results, that there can be strong features such as peaks in the measured intensity versus energy exchange, but in the quantum-mechanical regime we obtain a dependence on surface temperature that is quite different. There are additional features in the intensity that arise from a structure factor coming from the discrete periodic nature of the surface, and this structure disappears in the semiclassical limit. However, probably the most important result is the information on the interaction potential provided by the multiphonon background. Since the multiphonon background is the result of the exchange of many quanta, its form depends only very weakly on the specific nature of the surface-phonon spectral density. Instead the envelope of the multiphonon-background intensity gives the form factor, or the modulus of the transition matrix, for inelastic scattering. Using this inelastic form factor obtained from the multiphonon intensity, one can in principle extract the phonon spectral densities from the single-

phonon peak intensities.

Using simple methods for the phonon spectral density, a number of comparisons are made with experiments of the multiphonon background obtained in time-of-flight measurements of He scattering from alkali halide or metal surfaces. Good agreement is obtained for the behavior of the background structure as a function of surface temperature and momentum exchange. It is found that the form factor, or transition matrix, is very strongly dependent on momentum and energy exchange. There is a large difference in the inelastic scattering between alkali halides and metals, in both total scattering and in the distribution of scattering intensities in energy and momentum. The inelastic scattering from the alkali halide surfaces is substantially stronger, and this appears due to the much more rapid decay of the form factor as a function of energy and momentum exchange in the case of metals. It is this strongly varying behavior of the form factor that is a significant distinguishing feature of He scattering, as opposed to electron or x-ray probes for which the form factor is weakly dependent on the total momentum exchange.

II. DEVELOPMENT OF THEORY

The basic elements of the theory closely follow methods that have been introduced in studying neutron or x-ray scattering from bulk solids.[14–18] We briefly review the important features here and note the differences imposed by the configuration of scattering from a two-dimensional surface. The system is described by a Hamiltonian

$$H=H_0+V \ , \tag{1}$$

where H_0 is the sum of a free-particle Hamiltonian for the projectile and the unperturbed Hamiltonian of the solid

$$H_0=-\frac{\hbar^2}{2m}\nabla^2+H_0^c \ . \tag{2}$$

The eigenstates of H_0 are products of particle and crystal states

$$H_0|j\rangle=E_j|j\rangle=(E_j^p+E_j^c)|\mathbf{k}_j\rangle\,|n_j\rangle \ , \tag{3}$$

where j is the collective quantum number describing the particle momentum $\mathbf{k}_j$ and the set of crystal numbers n_j, and E_j is the total energy of the combined system

$$E_j=E_j^p+E_j^c=\frac{\hbar^2\mathbf{k}_j^2}{2m}+E_j^c \ , \tag{4}$$

with E_j^c the total energy of the unperturbed solid and E_j^p that of the particle.

All quantities measurable in a scattering event can be obtained from the transition rate

$$w_{fi}=\frac{2\pi}{\hbar}|\mathcal{T}_{fi}|^2\delta(E_f-E_i) \ , \tag{5}$$

where the $\mathcal{T}_{fi}$ are matrix elements taken with respect to unperturbed states of the transition operator $\mathcal{T}$, which obeys the equation

$$\mathcal{T}=V+VG^+\mathcal{T} \ , \tag{6}$$

where V is the interaction potential coupling the projectile to the solid. Since in an experiment only the initial and final state of the particle can be monitored, the measured quantity is the particle transition rate from $\mathbf{k}_i$ to $\mathbf{k}_f$, which is Eq. (5) summed over all final crystal states and averaged over initial crystal states,

$$w(\mathbf{k}_f,\mathbf{k}_i)=\frac{2\pi}{\hbar}\left\langle\!\!\left\langle \sum_{n_f}|\mathcal{T}_{fi}|^2\delta(E_f-E_i)\right\rangle\!\!\right\rangle \ . \tag{7}$$

The double brackets $\langle\!\langle\ \rangle\!\rangle$ represent the ensemble average over the crystal states.

Upon defining time-dependent operators in the interaction picture according to

$$\mathcal{T}(t)=e^{iH_0^c t/\hbar}\mathcal{T}e^{-iH_0^c t/\hbar} \ , \tag{8}$$

the particle transition rate can be written as the Fourier transform of the time-dependent correlation function[14,15]

$$w(\mathbf{k}_f,\mathbf{k}_i)=\frac{1}{\hbar^2}\int_{-\infty}^{+\infty}dt\,e^{-i(E_f^p-E_i^p)t/\hbar} \times\langle\!\langle n_i|\mathcal{T}_{\mathbf{k}_i,\mathbf{k}_f}(0)\mathcal{T}_{\mathbf{k}_f,\mathbf{k}_i}(t)|n_i\rangle\!\rangle \ , \tag{9}$$

where the notation $\mathcal{T}_{\mathbf{k}_f,\mathbf{k}_i}$ stands for matrix elements of the $\mathcal{T}$ operator of Eq. (6) taken with respect to the particle states $|\mathbf{k}_j\rangle$ of Eq. (3).

Equation (9) is a convenient starting point for the scattering of many types of particle probes from a collective system of matter. As an example, for the case of He scattering from surfaces, the experimental quantity usually measured is the differential reflection coefficient $dR/d\Omega_f\,dE_f^p$ giving the fraction of the incident particles which are scattered into a final solid angle of $d\Omega_f$ and energy interval dE_f^p. This is obtained from the transition rate (9) by dividing by the incident flux crossing a plane parallel to the surface, $j_i=\hbar k_{iz}/mL$ and multiplying by the density of available final particle states

$$\frac{d^2R}{d\Omega_f\,dE_f^p}=\frac{L^4}{(2\pi\hbar)^3}\frac{m^2|\mathbf{k}_f|}{k_{iz}}w(\mathbf{k}_f,\mathbf{k}_i) \ . \tag{10}$$

We adopt a notation in which the z direction is the outward-pointing normal from the surface, and vectors are divided into components parallel and perpendicular to the surface according to $\mathbf{k}_j=(\mathbf{K}_j,k_{jz})$. The quantity L is a quantization length set to unity.

It should be noted that the differential reflection coefficient of Eq. (10) is correct for the "standard" experimental configuration in which the incident beam illuminates a spot on the crystal and the acceptance angle of the detector includes the entire illuminated spot. In many time-of-flight configurations the situation is somewhat reversed, the illuminated spot can be considered large and the detector acceptance angle subtends only a small portion of the illuminated spot. For the latter configuration Eq. (10) is multiplied by $\cos\theta_i/\cos\theta_f$, where θ_f and θ_i are the incident and scattered polar angles, measured with respect to the normal to the surface.

We are now in a position to establish the major ap-

proximations upon which the remainder of this work is based. The first assumption will be that the transition operator can be written as a pairwise summation

$$\mathcal{T}=\sum_{l,\kappa}\tau^{l,\kappa}\ , \tag{11}$$

where l denotes surface unit cells and κ counts units of the basis within each unit cell. Included in κ is the counting of layers within the crystal unit cell. Thus l is a discrete two-dimensional variable and κ is discrete but three dimensional. The approximation of (11) neglects many-body forces which cannot be incorporated into pseudopotential form, but it does include multiple scattering within the unit cell and between different unit cells.

The second major approximation is to assume that all unit cells are identical and the surface is perfectly periodic, and then to write

$$\mathcal{T}_{\mathbf{k}_f,\mathbf{k}_i}(t)=\sum_{l,\kappa}e^{-\mathbf{k}\cdot[\mathbf{r}_{l,\kappa}+\mathbf{u}_{l,\kappa}(t)]}\tau^{\kappa}_{\mathbf{k}_f,\mathbf{k}_i}\ , \tag{12}$$

where $\mathbf{k}=\mathbf{k}_f-\mathbf{k}_i$ is the difference between incident and final wave vector, $\mathbf{r}_{l,\kappa}$ is the equilibrium position of the κth element of the lth unit cell, and $\mathbf{u}_{l,\kappa}(t)$ is the displacement about the equilibrium position. The form of Eq. (12) follows from (11) if $\exp\{\mathbf{k}\cdot\mathbf{u}_{l,\kappa}(t)\}$ commutes with τ. For the following we will make the more stringent assumption that τ is independent of the vibrational displacement $\mathbf{u}_{l,\kappa}(t)$.

The approximation of (12) is a perfectly natural one to make for the case of electron or x-ray scattering in which the scattering center is the atomic hard core, and even better for neutron scattering where the scattering center is the atomic nucleus. For the case of atom scattering, the potential is due largely to the correlation and exchange forces between the electron cloud of the incident atom and the electronic density of the surface. Then Eq. (12) is equivalent to assuming that the elements of the unit cell vibrate rigidly and are themselves not distorted by the vibrational motion. (Note that an element of the unit cell, in this usage, does not necessarily have to correspond to an actual atomic component of the cell; other divisions are possible and may be, under certain circumstances, convenient.) Nevertheless, the approximation of Eq. (12) should be good even for atom scattering in processes dominated by low-energy, long-wavelength phonons, such as the multiphonon-inelastic scattering emphasized here.

Inserting the transition operator in the form of Eq. (12) into the transition rate of (9) leads to

$$w(\mathbf{k}_i,\mathbf{k}_f)=\frac{1}{\hbar^2}\int_{-\infty}^{+\infty}dt\,e^{-i\omega t}\sum_{l,\kappa}\sum_{l',\kappa'}\tau^{\kappa}_{fi}\bar{\tau}^{\kappa'}_{fi}e^{-i\mathbf{k}\cdot(\mathbf{r}_{l,\kappa}-\mathbf{r}_{l',\kappa'})}\langle\langle n_i|e^{-i\mathbf{k}\cdot\mathbf{u}_{l,\kappa}(t)}e^{i\mathbf{k}\cdot\bar{\mathbf{u}}_{l',\kappa'}(0)}|n_i\rangle\rangle\ , \tag{13}$$

where we have used the shorthand notation $\tau_{fi}=\tau_{\mathbf{k}_f,\mathbf{k}_i}$ and $\omega=(E_f^p-E_i^p)/\hbar$.

The third major approximation is to assume that all vibrational displacements can be treated in the harmonic approximation. Then the average over crystal states can be carried out using well-known methods,[18] and the final form for the transition rate is

$$w(\mathbf{k}_i,\mathbf{k}_f)=\frac{1}{\hbar^2}\int_{-\infty}^{+\infty}dt\,e^{-i\omega t}\sum_{l,\kappa}\sum_{l',\kappa'}\tau^{\kappa}_{fi}\bar{\tau}^{\kappa'}_{fi}e^{-i\mathbf{k}\cdot(\mathbf{r}_{l,\kappa}-\mathbf{r}_{l',\kappa'})}e^{-W_{\kappa}(\mathbf{k})}e^{-W_{\kappa'}(\mathbf{k})}e^{\langle\langle n_i|\mathbf{k}\cdot\bar{\mathbf{u}}_{l',\kappa'}(0)\mathbf{k}\cdot\mathbf{u}_{l,\kappa}(t)|n_i\rangle\rangle}\ , \tag{14}$$

where

$$W_{\kappa}(\mathbf{k})=\tfrac{1}{2}\langle\langle n_i|\{\mathbf{k}\cdot\mathbf{u}_{l,\kappa}(t)\}^2|n_i\rangle\rangle\ , \tag{15}$$

is independent of l and t, and e^{-2W} is the classic expression for the Debye-Waller factor governing the decay of the scattered intensity as a function of target temperature.

Equation (14) is the starting point for the ensuing discussion of atom-surface scattering. The major approximation of Eq. (12) makes this a simpler expression in two important respects: (i) there has as yet been no need to specify an interaction potential describing the coupling between incoming projectile and surface, and (ii) the only time dependence appears in the exponentiated displacement correlation function $\langle\langle n_i|\mathbf{k}\cdot\bar{u}_{l',\kappa'}(0)\mathbf{k}\cdot\mathbf{u}_{l,\kappa}(t)|n_i\rangle\rangle$. Equation (14) can be easily related to more usual forms used in atom-surface scattering, notably the Born approximation and the distorted-wave Born approximation. In the Born approximation, with the interaction potential chosen to be a pairwise sum of interactions between the incident probe and the atoms of the target

$$V=\sum_{l,\kappa}v^{\kappa}(\mathbf{r}-\mathbf{r}_{l,\kappa}-\mathbf{u}_{l,\kappa})\ , \tag{16}$$

the transition rate is cast into exactly the form of (14) with τ^{κ}_{fi} equal to the Fourier transform of $v^{\kappa}(\mathbf{r})$. In the distorted-wave Born approximation, perturbation theory is developed starting from a distorting potential which back reflects all incident particles. In this case the transition rate again appears very similar to (14), but differs in two important respects: (i) τ_{fi} is replaced by a matrix element of the thermally averaged potential taken with respect to eigenstates of the distorting potential,[19] and (ii) the Debye-Waller factor contains only terms involving momentum transfer parallel to the surface. The contributions to the Debye-Waller thermal attenuation coming from momentum transfer perpendicular to the surface, which constitute by far the dominant contribution, come from higher-order terms in the distorted-wave perturbation series.[20,21]

As it stands the transition rate of Eq. (14) contains all possible phonon-exchange processes, both real and virtual. We can select out the elastic, single-quantum, and multiquantum processes by expanding the exponential of

the displacement correlation function to zeroth, first, and higher orders, respectively. In the next two sections we briefly discuss the elastic and single-quantum contribution, and in Sec. V we develop the multiphonon contribution.

III. ELASTIC SCATTERING

The transition rate for elastic scattering is obtained from (14) by replacing the exponential of the displacement correlation function by unity. Then

$$w^{(0)}(\mathbf{k}_i,\mathbf{k}_f)=\frac{2\pi}{\hbar}\delta(E_f^p-E_i^p)\sum_{l,\kappa}\sum_{l',\kappa'}\tau_{fi}^{\kappa}\bar{\tau}_{fi}^{\kappa'}e^{-i\mathbf{k}\cdot(\mathbf{r}_{l,\kappa}-\mathbf{r}_{l',\kappa'})}\times e^{-W_{\kappa}(\mathbf{k})}e^{-W_{\kappa'}(\mathbf{k})} . \tag{17}$$

The sum over unit cells gives rise to the diffraction conditions. Writing $\mathbf{r}_{l,\kappa}=\mathbf{R}_l+\mathbf{r}_{\kappa}$, where $\mathbf{R}_l$ is the vector parallel to the surface which denotes unit-cell positions, we have

$$\sum_{l,l'}e^{-i\mathbf{K}\cdot(\mathbf{R}_l-\mathbf{R}_{l'})}=N\sum_{l}e^{-i\mathbf{K}\cdot\mathbf{R}_l}=N^2\sum_{\mathbf{G}}\delta_{\mathbf{K},\mathbf{G}} , \tag{18}$$

where $\mathbf{G}$ is a surface reciprocal-lattice vector, and N is the number of surface unit cells. Then the elastic transition rate becomes

$$w^{(0)}(\mathbf{k}_i,\mathbf{k}_f)=\frac{2\pi}{\hbar}\sum_{\mathbf{G}}\delta_{\mathbf{K},\mathbf{G}}\delta(E_f^p-E_i^p)\times\left|\sum_{\kappa}\tau_{fi}^{\kappa}e^{-W_{\kappa}(\mathbf{k})}e^{-i\mathbf{k}\cdot\mathbf{r}_{\kappa}}\right|^2 . \tag{19}$$

The δ functions show that the elastic-scattering intensity is nonvanishing only when the conditions of conservation of energy and momentum parallel to the surface are satisfied. The intensity of each diffraction peak is governed by the squared amplitude in (19), which is a double sum over the elements of the unit-cell basis involving the scattering amplitude, scattering phase, and Debye-Waller factor. If the unit cell if a Bravais cell containing only one atom, then (19) reduces to

$$w^{(0)}(\mathbf{k}_i,\mathbf{k}_f)=\frac{2\pi}{\hbar}\sum_{\mathbf{G}}|\tau_{fi}|^2e^{-2W(\mathbf{k})}\delta_{\mathbf{K},\mathbf{G}}\delta(E_f^p-E_i^p) , \tag{20}$$

the standard form for the diffraction in which the intensity given by the product of a form factor, a Debye-Waller factor, and a structure factor.

IV. SINGLE-QUANTUM INELASTIC SCATTERING

The exchange of a single real phonon is described by expanding the exponential of the displacement correlation function in Eq. (14) to first order:

$$w^{(1)}(\mathbf{k}_i,\mathbf{k}_f)=\frac{1}{\hbar^2}\int_{-\infty}^{+\infty}dt\,e^{-i\omega t}\sum_{l,\kappa}\sum_{l',\kappa'}\tau_{fi}^{\kappa}\bar{\tau}_{fi}^{\kappa'}e^{-i\mathbf{k}\cdot(\mathbf{r}_{l,\kappa}-\mathbf{r}_{l',\kappa'})}e^{-W_{\kappa}(\mathbf{k})}e^{-W_{\kappa'}(\mathbf{k})}\langle\langle n_i|\mathbf{k}\cdot\bar{\mathbf{u}}_{l',\kappa'}(0)\mathbf{k}\cdot\mathbf{u}_{l,\kappa}(t)|n_i\rangle\rangle . \tag{21}$$

The αth Cartesian component of the surface-atomic-displacement operator can be expanded in the normal harmonic modes of the crystal.

$$\mathbf{u}_{l,\kappa}^{\alpha}(t)=\sum_{\mathbf{Q},\nu}\left[\frac{\hbar}{2NM_{\kappa}\omega_{\nu}(\mathbf{Q})}\right]^{1/2}e_{\alpha}\left[\kappa\left|\begin{matrix}\mathbf{Q}\\ \nu\end{matrix}\right.\right]e^{i\mathbf{Q}\cdot\mathbf{R}_{l,\kappa}}[a_{\nu}^{\dagger}(\mathbf{Q})e^{-i\omega_{\nu}(\mathbf{Q})t}+a_{\nu}(-\mathbf{Q})e^{i\omega_{\nu}(\mathbf{Q})t}] , \tag{22}$$

where M_{κ} is the mass of the κth surface atom, $\mathbf{Q}$ is the parallel wave vector, ν is a discrete quantum number for surface modes and continuous for bulk modes; $e_{\alpha}(\kappa|\begin{smallmatrix}\mathbf{Q}\\ \nu\end{smallmatrix})$ is the polarization vector of the $(\mathbf{Q},\nu)$ mode, $\omega_{\nu}(\mathbf{Q})$ is the mode frequency, and $a_{\nu}^{\dagger}(\mathbf{Q})$ is the creation operator. The sum over $\mathbf{Q}$ is limited to a single surface Brillouin zone.

The displacement correlation function now becomes

$$\langle\langle n_i|\mathbf{k}\cdot\bar{\mathbf{u}}_{l',\kappa'}(0)\mathbf{k}\cdot\mathbf{u}_{l,\kappa}(t)|n_i\rangle\rangle=\sum_{\alpha,\alpha'=1}^{3}k_{\alpha}k_{\alpha'}\sum_{\mathbf{Q},\nu}\frac{\hbar}{2N\sqrt{M_{\kappa}M_{\kappa'}}\omega_{\nu}(\mathbf{Q})}e_{\alpha}\left[\kappa\left|\begin{matrix}\mathbf{Q}\\ \nu\end{matrix}\right.\right]\bar{e}_{\alpha'}\left[\kappa'\left|\begin{matrix}\mathbf{Q}\\ \nu\end{matrix}\right.\right]e^{i\mathbf{Q}\cdot(\mathbf{R}_{l,\kappa}-\mathbf{R}_{l',\kappa'})}\times\{[n(\omega_{\nu}(\mathbf{Q}))+1]e^{-i\omega_{\nu}(\mathbf{Q})t}+n(\omega_{\nu}(\mathbf{Q}))e^{i\omega_{\nu}(\mathbf{Q})t}\} , \tag{23}$$

where $n(\omega_{\nu}(\mathbf{Q}))$ is the Bose-Einstein function

$$n(\omega_{\nu}(\mathbf{Q}))=\{e^{\hbar\omega_{\nu}(\mathbf{Q})/k_BT}-1\}^{-1} , \tag{24}$$

with T the temperature of the surface and k_B Boltzmann's constant.

Equation (23) allows us to immediately evaluate the Debye-Waller factor; the exponent $W_{\kappa}(\mathbf{k})$ is obtained from (23) in the limit $t\to 0$, $l=l'$, and $\kappa=\kappa'$:

$$W_{\kappa}(\mathbf{k})=\sum_{\alpha,\alpha'=1}^{3}k_{\alpha}k_{\alpha'}\sum_{\mathbf{Q},\nu}\frac{\hbar}{NM_{\kappa}\omega_{\nu}(\mathbf{Q})}e_{\alpha}\left[\kappa\left|\begin{matrix}\mathbf{Q}\\ \nu\end{matrix}\right.\right][n(\omega_{\nu}(\mathbf{Q}))+\tfrac{1}{2}] . \tag{25}$$

We note that the Debye-Waller factor can be a very important correction even under circumstances where $n(\omega)$ is small. This is because a surface-scattering experiment is a backscattering configuration and $k_z=|k_{fz}|+|k_{iz}|$ can be

rather large, which in turn makes $W_\kappa(\mathbf{k})$ large. On the other hand, the parallel momentum exchange $\mathbf{K}=\mathbf{K}_f-\mathbf{K}_i$ is often small in comparison to k_z and in many cases can be neglected.

Combining (25), (23), and (21), and carrying out the sums over l and l', the single-phonon transition rate is expressed as

$$w^{(1)}(\mathbf{k}_i,\mathbf{k}_f)=\pi N\sum_{\alpha,\alpha'=1}^{3}k_\alpha k_{\alpha'}\sum_{\kappa,\kappa'}\tau_{fi}^{\kappa}\bar{\tau}_{fi}^{\kappa'}e^{-W_\kappa(\mathbf{k})}e^{-W_{\kappa'}(\mathbf{k})}\frac{1}{\sqrt{M_\kappa M_{\kappa'}}\omega_\nu(\mathbf{K})}e^{-ik_z(z_\kappa-z_{\kappa'})}$$
$$\times\left[\sum_\nu e_\alpha\left[\kappa\middle|\frac{-\mathbf{K}}{\nu}\right]e_{\alpha'}\left[\kappa'\middle|\frac{-\mathbf{K}}{\nu}\right][n(\omega_\nu(\mathbf{K}))+1]\delta(E_f^p-E_i^p+\hbar\omega_\nu(\mathbf{K}))\right.$$
$$\left.+\sum_\nu e_\alpha\left[\kappa\middle|\frac{\mathbf{K}}{\nu}\right]\bar{e}_{\alpha'}\left[\kappa'\middle|\frac{\mathbf{K}}{\nu}\right]n(\omega_\nu(\mathbf{K}))\delta(E_f^p-E_i^p-\hbar\omega_\nu(\mathbf{K}))\right]. \tag{26}$$

Equation (26) shows that for the exchange of discrete surface modes (e.g., Rayleigh modes) the intensity appears as a sharp peak in an energy-resolved measurement. The term proportional to $n(\omega)+1$ is for phonon creation and the term proportional to $n(\omega)$ is for phonon annihilation. The transition rate is cast into a somewhat similar looking form using the standard definition of the phonon spectral density:[22]

$$\rho_{\kappa,\kappa'}^{\alpha,\alpha'}(\mathbf{K},\omega)=\sum_\nu\frac{\hbar}{2S_{\rm uc}\omega_\nu(\mathbf{K})\sqrt{M_\kappa M_{\kappa'}}}e_\alpha\left[\kappa\middle|\frac{\mathbf{K}}{\nu}\right]\bar{e}_{\alpha'}\left[\kappa'\middle|\frac{\mathbf{K}}{\nu}\right]\delta(\omega-\omega_\nu(\mathbf{K}))\,, \tag{27}$$

where $S_{\rm uc}$ is the surface area of the unit cell. Then (26) becomes

$$w^{(1)}(\mathbf{k}_i,\mathbf{k}_f)=\frac{2\pi NS_{\rm uc}}{\hbar}\sum_{\alpha,\alpha'=1}^{3}k_\alpha k_{\alpha'}\sum_{\kappa,\kappa'}\tau_{fi}^{\kappa}\bar{\tau}_{fi}^{\kappa'}e^{-W_\kappa(\mathbf{k})}e^{-W_{\kappa'}(\mathbf{k})}e^{-ik_z(z_\kappa-z_{\kappa'})}\{\rho_{\kappa,\kappa'}^{\alpha,\alpha'}(-\mathbf{K},\omega)[n(\omega)+1]+\rho_{\kappa,\kappa'}^{\alpha,\alpha'}(\mathbf{K},\omega)n(\omega)\}\,. \tag{28}$$

We note that in the transition rates of (26) or (28) the major influence of the interaction between the incoming probe and the surface is contained in the scattering amplitudes τ_{fi} which are not yet specified. However, just as for the elastic case, connection can be made with previous calculations based on perturbation theory. In the Born approximation, with a pairwise summation of potentials, the only change in (28) is that τ_{fi} becomes the Fourier transformation of the pairwise potential. In the distorted-wave Born approximation, τ_{fi} becomes a matrix element of the thermally averaged potential taken with respect to distorted states, and in addition the Debye-Waller factor must be introduced through supplementary considerations.[20,21] An advantage of the expression (28) is its ability to directly relate the single-phonon and multiphonon contributions, as discussed in the next section, and its use for discussing single-phonon scattering from surfaces with complicated unit cells.

It is of interest to look at the simplest possible situation, scattering from a surface Bravais cell, which in this case means only the outermost surface layer is considered, and the surface cell contains only one atom. Then the transition rate appears as

$$w^{(1)}(\mathbf{k}_i,\mathbf{k}_f)=\frac{2\pi NS_{\rm uc}}{\hbar}|\tau_{fi}|^2e^{-2W(\mathbf{k})}\sum_{\alpha,\alpha'=1}^{3}k_\alpha k_{\alpha'}\{\rho^{\alpha,\alpha'}(-\mathbf{K},\omega)[n(\omega)+1]+\rho^{\alpha,\alpha'}(\mathbf{K},\omega)n(\omega)\}\,. \tag{29}$$

This has reduced to the standard form for a single-quantum scattering process, the product of a form factor describing the envelope of scattering by a single unit cell, a Debye-Waller factor giving the thermal attenuation, a structure factor that is the phonon spectral density, and the Bose-Einstein factor for the number of phonons of the given frequency.

The form of the transition rate in Eq. (28) is very useful in describing the scattering from more complicated surfaces (e.g., stepped or reconstructed surfaces) having unit cells with a basis. For the case of atom scattering, the repulsive hard core of the potential plays the major role in elastic scattering, and it is usually sufficient to consider the interaction to be with only the outermost layer. (This condition is usually not satisfied by electron or x-ray scattering.) If we consider the further simplifying assumption that all atoms within the surface unit-cell layer scatter similarly, i.e., their amplitudes τ_{fi} and Debye-Waller factors are the same, then the transition rate appears as

$$w^{(1)}(\mathbf{k}_i,\mathbf{k}_f)=\frac{2\pi NS_{\rm uc}}{\hbar}|\tau_{fi}|^2 e^{-2W(\mathbf{k})}\sum_{\alpha,\alpha'=1}^{3}k_\alpha k_{\alpha'}\sum_{\kappa,\kappa'}e^{-ik_z(z_\kappa-z_{\kappa'})}\{\rho^{\alpha,\alpha'}_{\kappa,\kappa'}(-\mathbf{K},\omega)[n(\omega)+1]+\rho^{\alpha,\alpha'}_{\kappa,\kappa'}(\mathbf{K},\omega)n(\omega)\}\ . \quad (30)$$

This expression shows that such a scattering experiment cannot measure the phonon spectral density of a single atom, as in the case of a Bravais cell. Instead, what is measured is a double summation over all elements of the cell. This is given by the more complicated spectral density of the unit cell[23] given by

$$\rho^{\alpha,\alpha'}_{\rm uc}(\mathbf{K},\omega)=\sum_{\kappa,\kappa'}e^{-ik_z(z_\kappa-z_{\kappa'})}\rho^{\alpha,\alpha'}_{\kappa,\kappa'}(\mathbf{K},\omega)\ . \quad (31)$$

Inserting (31) into (30) leads to an expression for the transition rate which looks identical to (29) with $\rho^{\alpha,\alpha'}$ replaced by $\rho^{\alpha,\alpha'}_{\rm uc}$. Note that there is a phase relation in the summation of Eq. (31) depending on the relative vertical heights z_κ of the components of the unit cell. Even though we have considered only the outermost surface layer, the surface-cell atoms can still be at different heights with respect to the surface plane, and even if these relative heights are small, the phase can be important since k_z is often rather large.

Certainly, the assumption that all atoms in the unit cell scatter similarly is not always valid, an example to the contrary being vicinal stepped surfaces. In stepped surfaces it has been demonstrated in the case of He projectiles that the scattering characteristics of the step edges are quite different from that of the flat terraces between steps.[24] This fact, together with the strong dependence on scattering phase, can be used to selectively sample individual components of the unit cell. Following the very illuminating and useful construction applied by Hinch and Toennies[25] to elastic scattering from steps, we write the scattering amplitude of a terrace atom in the usual form τ_{fi}, but we characterize the different scattering amplitude of an edge atom, denoted here by $\kappa=0$, through an additive term,

$$e^{-W_0(\mathbf{k})}\tau^0_{fi}=e^{-W(\mathbf{k})}(\tau_{fi}+\delta_{fi})\ . \quad (32)$$

Then the transition rate (28) appears as

$$w^{(1)}(\mathbf{k}_i,\mathbf{k}_f)=\frac{2\pi NS_{\rm uc}}{\hbar}n(\omega)e^{-2W(\mathbf{k})}\sum_{\alpha,\alpha'=1}^{3}k_\alpha k_{\alpha'}\left[|\tau_{fi}|^2\sum_{\kappa,\kappa'=1}e^{-k_z(z_\kappa-z_{\kappa'})}\rho^{\alpha,\alpha'}_{\kappa,\kappa'}(\mathbf{K},\omega)\right.$$
$$\left.+2\,{\rm Re}\bar{\tau}_{fi}\delta_{fi}\sum_{\kappa=1}e^{-ik_z(z_\kappa-z_0)}\rho^{\alpha,\alpha'}_{\kappa,0}(\mathbf{K},\omega)+|\delta_{fi}|^2\rho^{\alpha,\alpha'}_{0,0}(\mathbf{K},\omega)\right]\ , \quad (33)$$

where we have written only the energy-gain (phonon-annihilation) term, and have assumed that all terrace atoms scatter similarly.

Equation (33) writes the scattering as a "terrace" contribution in $|\tau_{fi}|^2$, an "edge" contribution in $|\delta_{fi}|^2$, and an interference between the two. However, the behavior of τ_{fi} and δ_{fi} are quite different; $|\tau_{fi}|^2$ is a strongly varying function of $\mathbf{k}$ with a sharp peak in the neighborhood of the specular direction or in the rainbow direction relative to the terraces. The edge-atom form factor $|\delta_{fi}|^2$ scatters much more uniformly in all directions, with possibly a weak maximum in the rainbow direction relative to the step faces. (This behavior is clear in the experimental data for elastic scattering[25,26] and has been demonstrated in calculations for inelastic scattering.[27]) Thus Eq. (33) shows that one can selectively obtain information on the spectral density of the edge atoms or of the terraces by choosing incident parameters (incident angle, scattering angle, and incident energy) in order to ensure a scattering configuration such that $|\delta_{fi}|^2$ is large and $|\tau_{fi}|^2$ is small, or vice versa.

V. MULTIPLE-QUANTUM SCATTERING

Now that the elastic and single-phonon contributions have been developed in the sections above, it is a straightforward matter to write down the multiphonon contribution. It is given by Eq. (14) with the zero- and single-quantum terms subtracted off,

$$w(\mathbf{k}_i,\mathbf{k}_f)=\frac{1}{\hbar^2}\int_{-\infty}^{+\infty}dt\,e^{-i\omega t}\sum_{l,\kappa}\sum_{l',\kappa'}\tau^{\kappa}_{fi}\bar{\tau}^{\kappa'}_{fi}e^{-i\mathbf{k}\cdot(\mathbf{r}_{l,\kappa}-\mathbf{r}_{l',\kappa'})}e^{-W_\kappa(\mathbf{k})}e^{-W_{\kappa'}(\mathbf{k})}$$
$$\times[e^{\langle\langle n_i|\mathbf{k}\cdot\bar{\mathbf{u}}_{l',\kappa'}(0)\mathbf{k}\cdot\mathbf{u}_{l,\kappa}(t)|n_i\rangle\rangle}-1-\langle\langle n_j|\mathbf{k}\cdot\bar{\mathbf{u}}_{l',\kappa'}(0)\mathbf{k}\cdot\mathbf{u}_{l,\kappa}(t)|n_i\rangle\rangle]\ . \quad (34)$$

For multiphonon exchange it is most convenient to write the displacement correlation function (23) in the form

$$\langle\langle n_i|\mathbf{k}\cdot\bar{\mathbf{u}}_{l',\kappa'}(0)\mathbf{k}\cdot\mathbf{u}_{l,\kappa}(t)|n_i\rangle\rangle=\sum_{\alpha,\alpha'=1}^{3}k_\alpha k_{\alpha'}\sum_{\mathbf{Q},\nu}\frac{\hbar}{2N\sqrt{M_\kappa M_{\kappa'}}\omega_\nu(\mathbf{Q})}e_\alpha\left[\kappa\left|\begin{matrix}\mathbf{Q}\\ \nu\end{matrix}\right.\right]\bar{e}_{\alpha'}\left[\kappa'\left|\begin{matrix}\mathbf{Q}\\ \nu\end{matrix}\right.\right]e^{i\mathbf{Q}\cdot(\mathbf{R}_{l,\kappa}-\mathbf{R}_{l',\kappa'})}$$
$$\times\{[2n(\omega_\nu(\mathbf{Q}))+1]\cos[\omega_\nu(\mathbf{Q})t]-i\sin[\omega_\nu(\mathbf{Q})t]\}\ . \quad (35)$$

In practice Eqs. (34) and (35) can be used as the starting point for a completely numerical calculation of the multiphonon scattering. The time-dependent displacement correlation function (34) can be evaluated by using any standard calculational method for surface vibrations, e.g., a slab calculation[28] or Green-function's methods.[29] Then the Fourier transform over time in (34) is well behaved and can be carried out. More importantly the sum over lattice positions in (34) converges rapidly, as we show in the section below, and usually only a few terms are needed.

In the simplest case of a Bravais unit cell, the multiphonon transition rate of Eq. (34) is again the product of a form factor $|\tau_{fi}|^2$, a Debye-Waller factor, and a structure factor which reflects the periodic nature of the surface. It is of interest to emphasize that, within the approximations used here, the form factor is identical to that for single-phonon scattering, as seen, for example, in Eq (29). This implies that measurements of both the single-phonon intensity and the multiphonon background provide sufficient information to unambiguously determine both the form factor and the spectral density independently. Measurements of the single-phonon intensity alone are not sufficient for this, since the form factor is always multiplied by the spectral density, and only the product can be determined by measurement.

VI. MODEL CALCULATIONS

The multiphonon contribution can be explicitly evaluated for several simple phonon lattice-vibrational models. We exhibit here several of these forms in the correspondence limit of large numbers of phonons, while still retaining the quantum-mechanical nature of the projectile motion.

To begin, we adopt the case of a Bravais unit cell with only the surface layer contributing to inelastic scattering. In the correspondence limit in which large numbers of low-energy, long-wavelength phonons are transferred, the exponential in the displacement correlation function (35) can be expanded

$$\langle\langle n_i|\mathbf{k}\cdot\bar{\mathbf{u}}_{l+l'}(0)\mathbf{k}\cdot\mathbf{u}_l(t)|n_i\rangle\rangle=\sum_{\alpha,\alpha'=1}^{3}k_\alpha k_{\alpha'}\sum_{\mathbf{Q},\nu}\frac{\hbar}{2NM\omega_\nu(\mathbf{Q})}e_\alpha\begin{bmatrix}\mathbf{Q}\\ \nu\end{bmatrix}\bar{e}_{\alpha'}\begin{bmatrix}\mathbf{Q}\\ \nu\end{bmatrix}[1+i\mathbf{Q}\cdot\mathbf{R}_l-\tfrac{1}{2}(\mathbf{Q}\cdot\mathbf{R}_l)^2-i\tfrac{1}{6}(\mathbf{Q}\cdot\mathbf{R}_l)^3+\cdots]$$
$$\times\{[2n(\omega_\nu(\mathbf{Q}))+1]\cos[\omega_\nu(\mathbf{Q})t]-i\sin[\omega_\nu(\mathbf{Q})t]\}\ . \tag{36}$$

Due to symmetry, terms which are odd in Cartesian components of $\mathbf{Q}$ will vanish upon integration, and up to fourth order in the expansion, only the zeroth-order term and that in $(\mathbf{Q}\cdot\mathbf{R}_1)^2$ survive.

Also consistent with the correspondence limit is a first-order expansion of the sine and cosine functions in (36), leading to

$$\langle\langle n_i|\mathbf{k}\cdot\bar{\mathbf{u}}_{l'+l}(0)\mathbf{k}\cdot\mathbf{u}_l(t)|n_i\rangle\rangle=\sum_{\alpha,\alpha'=1}^{3}k_\alpha k_{\alpha'}\sum_{\mathbf{Q},\nu}\frac{\hbar}{2NM\omega_\nu(\mathbf{Q})}e_\alpha\begin{bmatrix}\mathbf{Q}\\ \nu\end{bmatrix}\bar{e}_{\alpha'}\begin{bmatrix}\mathbf{Q}\\ \nu\end{bmatrix}$$
$$\times\{-i\omega_\nu(\mathbf{Q})t+[2n(\omega_\nu(\mathbf{Q}))+1][\cos(\omega_\nu(\mathbf{Q})t)-\tfrac{1}{2}(\mathbf{Q}\cdot\mathbf{R}_l^2)]\}\ . \tag{37}$$

Inserting (37) back into the transition rate of Eq. (34) (ignoring for the moment the extraction of zero- and one-quantum terms) leads to the following form:

$$w(\mathbf{k}_f,\mathbf{k}_i)=\frac{N}{\hbar^2}|\tau_{fi}|^2e^{-2W(\mathbf{k})}S(\mathbf{K},\omega)I(\mathbf{K},\omega)\ , \tag{38}$$

where

$$S(\mathbf{K},\omega)=\sum_l e^{-i\mathbf{K}\cdot\mathbf{R}_l}e^{-F_l} \tag{39}$$

with

$$F_l=\sum_{\alpha,\alpha'=1}^{3}k_\alpha k_{\alpha'}\sum_{\mathbf{Q},\nu}\frac{\hbar(\mathbf{Q}\cdot\mathbf{R}_l)^2}{2NM\omega_\nu(\mathbf{Q})}\times e_\alpha\begin{bmatrix}\mathbf{Q}\\ \nu\end{bmatrix}\bar{e}_{\alpha'}\begin{bmatrix}\mathbf{Q}\\ \nu\end{bmatrix}[2n(\omega_\nu(\mathbf{Q}))+1]\ , \tag{40}$$

and

$$I(\mathbf{K},\omega)=\int_{-\infty}^{+\infty}dt\,e^{-i(\omega+\omega_0)t}e^{Q(t)}\ , \tag{41}$$

with

$$Q(t)=\sum_{\alpha,\alpha'=1}^{3}k_\alpha k_{\alpha'}\sum_{\mathbf{Q},\nu}\frac{\hbar}{2NM\omega_\nu(\mathbf{Q})}\times e_\alpha\begin{bmatrix}\mathbf{Q}\\ \nu\end{bmatrix}\bar{e}_{\alpha'}\begin{bmatrix}\mathbf{Q}\\ \nu\end{bmatrix}[2n(\omega_\nu(\mathbf{Q}))+1]\times\cos[\omega_\nu(\mathbf{Q})t]\ , \tag{42}$$

and

$$\omega_0=\frac{\hbar k^2}{2M}\ . \tag{43}$$

In the limit $t\to 0$, $Q(t)$ is just the Debye-Waller exponent of Eq. (25), and F_l is a closely related sum in which the summand is weighted by the square of the parallel momentum.

The transition rate of Eq. (38) is the product of a form factor $|\tau_{fi}|^2$, a Debye-Waller factor, a structure factor $S(\mathbf{K},\omega)$ arising from the periodic distribution of surface atoms, and an energy exchange factor $I(\mathbf{K},\omega)$. The structure factor is a rapidly convergent sum over lattice

sites, since Eq. (40) shows that F_l varies as $\mathbf{R}_l^2$.

The energy shift ω_0 appearing in the Fourier transform or energy transfer factor of (41) has its origins in the zero-point motion of the lattice, as is evident from Eq. (35) or (36). It is interesting that even though the zero-point motion is usually considered a low-temperature effect, here it has an important manifestation in the extreme semiclassical limit of high temperature and incident energy. In this limit $\hbar\omega_0$ is the average energy given up to the surface. The importance of the zero-point motion in this context is noted even in the case of high-energy ion scattering.[9,30,31]

We can evaluate $Q(t)$ in the high-temperature limit, where $n(\omega)\rightarrow\hbar\omega/k_BT$, by assuming an isotropic, dispersionless phonon distribution in which the frequency and wave vector are related by $\omega=ck$, where c is the sound velocity, and this is equivalent to a three-dimensional Debye phonon distribution. Interference terms between different Cartesian components of the phonon polarization vectors are zero, and the result is

$$Q(t)=\frac{3\mathbf{k}^2k_BT}{M\omega_D^3}\frac{\sin(\omega_Dt)}{t}\ , \tag{44}$$

where ω_D is the Debye frequency. The familiar expression for the Debye-Waller exponent (25) is obtained from (45) by setting $t\rightarrow 0$,

$$2W(\mathbf{k})=\frac{3\mathbf{k}^2k_BT}{M\omega_D^2}=\frac{6\omega_0k_BT}{\hbar\omega_D^2}\ . \tag{45}$$

The summand in Eq. (40) for F_l involves the momentum transfer parallel to the surface, and following the lead of previous work,[6-8] we can evaluate this expression for a two-dimensional dispersionless and isotropic surface mode in which $\omega=v_RK$ and v_R can be taken as a parameter roughly equal to the Rayleigh phonon velocity. This is equivalent to a two-dimensional Debye model with the two-dimensional Debye frequency related to v_R by

$$\omega_{2D}^2=4\pi v_R^2/S_{uc}\ . \tag{46}$$

The result is

$$F_l=\frac{\omega_0k_BT\mathbf{R}_l^2}{2\hbar v_R^2}\ . \tag{47}$$

With the Debye-model evaluation of Eqs. (44), (45), and (47), the transition rate in the correspondence limit of large numbers of quantum exchange and large T takes the final form

$$w(\mathbf{k}_f,\mathbf{k}_i)=\frac{N}{\hbar^2}|\tau_{fi}|^2e^{-2W(\mathbf{k})}\times\sum_l e^{-i\mathbf{K}\cdot\mathbf{R}_l}\exp\left[\frac{-\omega_0k_BT\mathbf{R}_l^2}{2\hbar v_R^2}\right]\times\int_{-\infty}^{+\infty}dt\,e^{-i(\omega+\omega_0)t}\times\exp\left[2W(\mathbf{k})\frac{\sin(\omega_Dt)}{\omega_Dt}\right]\ . \tag{48}$$

Expression (48), with zero- and single-quantum contributions subtracted out, has been used in all of the comparisons with experiment carried out in the next section. The structure factor involving the sum over lattice sites has been evaluated by direct numerical summation. The Fourier transform in time can be carried out by direct numerical integration, but we have found it most efficient to expand the integrand to high order and carry out the integral term by term using the well-known Fourier transform of $[(\sin x)/x]^n$. Both methods give identical results.

It is of interest to discuss the form of the structure factor appearing in (48), which we write as

$$S(\mathbf{K},\omega)=\sum_l e^{-i\mathbf{K}\cdot\mathbf{R}_l}e^{-F(k)R_l^2/a^2}\ , \tag{49}$$

where $F(\mathbf{k})=\omega_0k_BTa^2/2\hbar v_R^2$, with a taken as a convenient length comparable to the lattice spacing. This has the appearance of the structure factor for elastic diffraction, but the summand is modified by a Gaussian damping function depending on T and total momentum exchange k. $S(\mathbf{K},\omega)$ is peaked at values of $\mathbf{K}$ equal to the reciprocal lattice vectors $\mathbf{G}$, and near these positions can be approximated by a Gaussian function. For nonsimple surface unit cells, such as that of the fcc (111) surface, $S(\mathbf{K},\omega)$ may exhibit additional structure between the diffraction peak positions. In the extreme semiclassical limit of high T and large k, $S(\mathbf{K},\omega)=1$ and only a single term in the summation over lattice sites contributes. This behavior is quite physical: It implies that the multiphonon intensity can be associated with the diffraction peak positions, and the coherent region of the crystal surface which contributes to the multiphonon signal is roughly of area $a^2/F(\mathbf{k})$. In the extreme semiclassical limit, $F(\mathbf{k})\gg 1$, the association with diffraction peak positions is lost, and the coherence area shrinks to zero implying that the multiphonon intensity arises essentially from scattering with a single-surface atom. Thus in this extreme semiclassical limit, the structure factor for scattering from a perfectly ordered surface is no different from the structure factor associated with an isolated defect, and the only difference between the coherent and incoherent multiphonon intensity distribution will be due to the difference in form factor.

VII. THE SEMICLASSICAL LIMIT

There have been several recent and interesting treatments of semiclassical and classical-trajectory approximations to the multiphonon scattering of atomic and molecular particles at surfaces,[6-11] as well as treatments based on numerical calculations.[12,13] It is of interest to consider the present theory in this limit as it leads to closed-form expressions for the scattering intensities, and gives criteria for the validity of the extreme semiclassical limit.[6-10]

For the energy exchange factor the semiclassical limit is obtained by carrying out the Fourier transform in Eq. (41) by the method of steepest descents. This is effected by expanding $Q(t)$ of Eq. (42) to order t^2, and the result in the Debye model of Eq. (44) is

$$I(\mathbf{K},\omega)=e^{2W(\mathbf{k})}\left[\frac{\hbar\pi}{\omega_0 k_B T}\right]^{1/2}\exp\left[-\frac{\hbar(\omega+\omega_0)^2}{4k_B T\omega_D}\right]. \quad (50)$$

The Debye-Waller factor is cancelled, and the energy exchange in this limit is a Gaussian function of the energy exchanged, but shifted to the energy-loss side by the amount $\hbar\omega_0$. The width of the energy exchange function is roughly $2\sqrt{k_B T\hbar\omega_D}$ in energy units, and the peak amplitude decays with increasing temperature as $(k_B T\hbar\omega_0)^{-1/2}$.

The steepest-descent evaluation of Eq. (50) also implies a criterion for the validity of the semiclassical result,

$$2W(\mathbf{k})/6 \gg 1 . \quad (51)$$

This is a very stringent criterion, and is in fact rarely satisfied in typical He-scattering experiments, and often not satisfied even when the projectile is a heavier atom such as Ne or Ar. Note that as discussed above, the average number of phonons exchanged in a collision process is approximately equal to $2W$, thus (51) implies that for the semiclassical approximation to be valid, a truly large number of quanta must be exchanged. In practice we find that for $2W<6$ the energy transfer factor of (50) differs strongly from Gaussian form and is an increasing (rather than decreasing) function of T. For values of $2W\geq 6$ the Gaussian form of Eq. (50) is a reasonable approximation.

A semiclassical approximation to the structure factor has been developed[6-8] that has the form of a Gaussian in parallel momentum transfer. We can obtain this limit from the structure factor of (49) by approximating the summation over lattice sites by an integral. The result for a square surface unit cell of dimension a is

$$S(\mathbf{K},\omega)=\frac{\pi}{F(\mathbf{k})}\exp\left[\frac{-K^2a^2}{4F(\mathbf{k})}\right]$$
$$=\frac{2\pi\hbar v_R^2}{a^2\omega_0 k_B T}\exp\left[\frac{-2\hbar v_R^2 K^2}{4\omega_0 k_B T}\right]. \quad (52)$$

This is essentially a Gaussian function of K having the same width dependence as the energy exchange function (50), and with a peak value which decreases with temperature as $1/k_B T\hbar\omega_0$.

There is a definite problem with the approximate form for $S(\mathbf{K},\omega)$ of Eq. (52). The validity of the transition from sum to integral depends on $F(\mathbf{k})$ being smaller than unity, while the approximations leading to the original summation form of Eq. (49) depend on the semiclassical condition $F(\mathbf{k})\gg 1$. Thus there is a very narrow range of validity in which Eq. (52) can be considered a reasonable approximation for the structure factor. Clearly the approximation of Eq. (52) does not exhibit the periodicity inherent in Eq. (49), but the most striking difference is in the temperature dependence. The summation over lattice sites in (49) becomes exact in the semiclassical limit and approaches a constant, while the approximation of (52) decreases as $1/T$.

The semiclassical transition rate based on the approximations of Eqs. (50) and (52) is

$$w^{\mathrm{sc}}(\mathbf{k}_f,\mathbf{k}_i)=\frac{2N}{\hbar^2}|\tau_{fi}|^2 v_R^2\left[\frac{\hbar\pi}{\omega_0 k_B T}\right]^{3/2}$$
$$\times\exp\left[-\frac{\hbar(\omega+\omega_0)^2+2\hbar v_R^2 K^2}{4k_B T\omega_0}\right]. \quad (53)$$

This, with $|\tau_{fi}|^2$ taken to be constant is essentially the expression developed by Brako and Newns[7] and can be arrived at by purely classical thermodynamical treatments of scattering from an isotropic continuum surface.[8] The choice of ω_0 often made in a semiclassical treatment is the Baule expression derived from binary particle collisions, modified by the presence of the attractive well:

$$\hbar\omega_0\simeq\frac{4\mu}{(1+\mu)^2}(E_i^p\cos^2\theta_i+D), \quad (54)$$

where $\mu=m/M$ is the ratio of projectile to surface-atom mass, and D is the depth of the attractive potential well in front of the surface. The present treatment gives a natural evaluation for ω_0 in Eq. (43), which in the semiclassical limit where $k_{fz}\simeq k_{iz}$ is very close to (54), namely

$$\hbar\omega_0\simeq\frac{4\hbar^2 k_{iz}^2}{2M}=4\mu E_i^p\cos^2\theta_i , \quad (55)$$

differing from the Baule expression only the absence in the denominator of the factor $(1+\mu)^2$. We could readily include the well depth D in our treatment by using the same arguments inherent in (54), that the attractive part of the particle surface potential is rigid (and consequently does not contribute to inelastic exchange) and is sufficiently smoothly varying that it also does not elastically backscatter an appreciable fraction of the incident particle amplitude.[32-34]

There is a clear difference between the semiclassical result of Eq. (53), and the present result of Eq. (48) expressed in the semiclassical limit. The semiclassical limit of Eq. (48) makes use of (50), but the strucutre factor becomes a constant, thus

$$w(\mathbf{k}_f,\mathbf{k}_i)\rightarrow\frac{N}{\hbar^2}|\tau_{fi}|^2\left[\frac{\hbar\pi}{\omega_0 k_B T}\right]^{1/2}\exp\left[-\frac{\hbar(\omega+\omega_0)^2}{4k_B T\omega_0}\right]. \quad (56)$$

The temperature dependence of the peak intensity varies as $1/\sqrt{T}$ as opposed to $1/T^{3/2}$ in (53), and there is no dependence on parallel momentum in the exponential.

In calculations for comparison with experimental data discussed in the next section, we have found that Eq. (56) is usually not even approximately valid for the scattering of He atoms. With typical He incident energies in the 10–100-meV range, the behavior of (56) is recovered only at surface temperatures several times the bulk Debye temperature Θ_D. On the other hand, the transition rate of Eq. (48) agrees well with experimental data taken at temperatures even smaller than Θ_D, and it is found that the multiphonon intensity typically increases with temperature at values of T comparable to Θ_D.

VIII. COMPARISON WITH EXPERIMENT

An excellent experimental test of the theories developed here for multiple-quantum inelastic interactions is the scattering of He by surfaces. In typical experiments where incident wave vectors range between 5 and 20 Å^{-1}, the de Broglie wavelength is of the order of 1 Å, and hence the motion of the He probe is quantum mechanical. With surface temperatures ranging from T less than Θ_D to several times Θ_D, the inelastic background is characterized by the average number of exchanged quanta $2W(\mathbf{k})$ which ranges from the purely quantum-mechanical, single-phonon limit up to about 10.

We choose the widely disparate examples of He scattering by alkali halide insulators and by close-packed metal surfaces. The alkali halides are strong inelastic scatterers, while close-packed metal surfaces are weak inelastic scatterers because they are very flat and have a relatively soft repulsive potential.

In order to make quantitative comparisons with experiment, the scattering amplitude τ_{fi}, or rather the form factor $|\tau_{fi}|^2$ must be specified. This has been extensively studied in previous work explaining the intensities of single-phonon inelastic peaks.[35,36] Harten *et al.* have found, through a careful consideration of pairwise summation potentials for the He-surface interaction V, that $|\tau_{fi}|^2$ can be expressed as the product of a cutoff function in parallel momentum $\mathbf{K}$ and the Mott-Jackson matrix element[35,36] in the perpendicular momentum:

$$|\tau_{fi}|^2 = e^{-2K^2/Q_c^2} v_{\mathrm{MJ}}^2(k_{fz},k_{iz}) \ . \tag{57}$$

The Mott-Jackson factor is the matrix element of the one-dimensional potential $v(z)=e^{-\beta z}$ taken with respect to its own distorted eigenstates. The form factor (57) is then normalized to unity for specular scattering, has exponential decay in K^2, and the Mott-Jackson factor behaves roughly as an exponential decay in the normal momentum difference $|k_{fz}-k_{iz}|$. The two parameters Q_c and β are best known for metal surfaces where it is found that the cutoff momentum Q_c is around 1 Å^{-1}, while the range parameter β is usually somewhat larger than 2 Å^{-1}. In all of the following comparisons we adopt (57) for the scattering form factor of the surface unit cell.

Recently Skofronick *et al.*[37–39] have carried out extensive investigations of both single-phonon and multiphonon scattering of He by alkali halides. Figure 1 shows an energy-resolved scan of the scattering of 44-meV He beam from a NaCl(001) surface in the ⟨100⟩ azimuthal direction at two different temperatures, 673 and 523 K. The experiment is a so-called "specular" scan configuration in which $\theta_i=\theta_f$ and in this case θ_i is 45°. The increasing amount of background noise on the energy-loss side is simply an artifact of the conversion from the experimentally measured time-of-flight intensities to the energy exchange scale.

The solid curve in Fig. 1 is the theoretical result given by the differential reflection coefficient of Eq. (10) using the transition rate of Eq. (48) and the form factor of Eq. (57). The effective Debye temperature is determined by comparison of measurements of the specular intensity with the Debye-Waller factor of Eq. (45) and is 224 K.

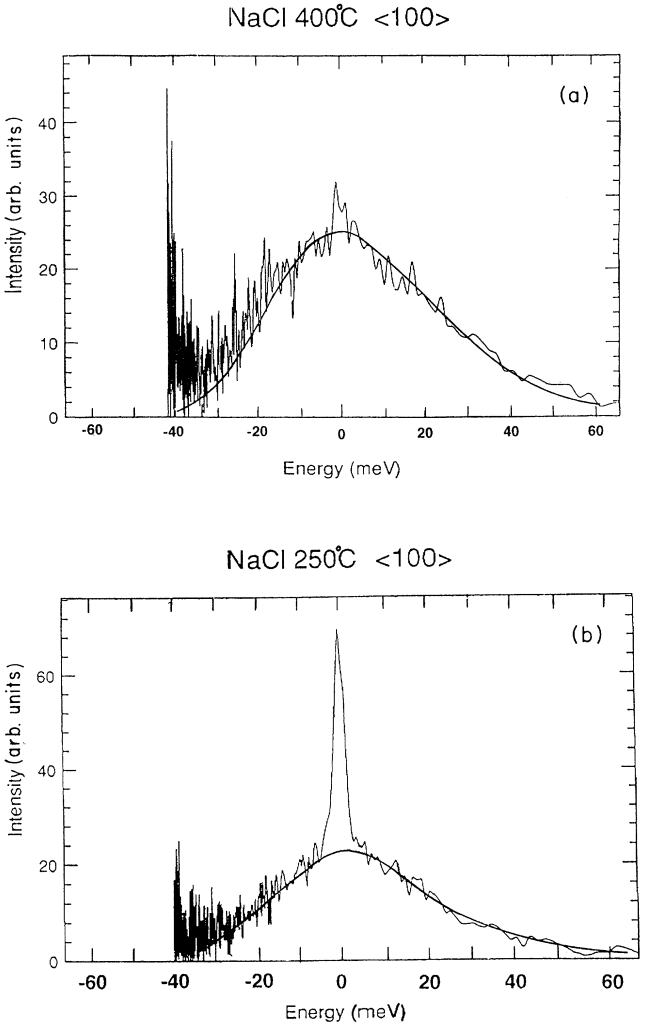

FIG. 1. The scattered intensity as a function of energy exchange for He on a NaCl(001) surface in the ⟨100⟩ direction. The incident beam wave vector is 9.2 Å^{-1}, and the angle of incidence and the detector angle are both 45°, measured from the surface normal. The solid curve is the calculation. (a) Surface temperature of 673 K. (b) Surface temperature of 523 K.

The cutoff parameter is $Q_c=5$ Å^{-1} and the range parameter is $\beta=6$ Å^{-1}, which is a very weak dependence of the form factor on the energy and momentum exchange. The value of v_R is unimportant, as the structure factor $S(\mathbf{K},\omega)$ is essentially unity even for temperatures of order Θ_D.

The agreement between theory and experiment is excellent, and this agreement extends to all temperatures measured, from $T\simeq 200$ to 800 K. There is a small increase in the multiphonon background with T, and a small, nearly linear increase with T in the full width at half maximum of the multiphonon intensity; both of these behaviors agree well with theoretical calculations.[40] Note that the two extreme semiclassical results (53) and (56) would predict a decrease in inelastic intensity with T,

and a $\sqrt{T}$ dependence for the width, clearly in disagreement with experiment. For the higher temperature of 623 K, the value of $2W$ is about 4 (implying about 4 real phonons exchanged per collision), and the energy shift $\hbar\omega_0$ is about 10 meV. This energy shift, although arising from zero-point motion, is clearly non-negligible; without it the experimental and calculated curves cannot be made to agree regardless of how the parameters are varied.

Figure 2 shows a similar comparison of He scattering by the NaCl(001) surface, except now for the ⟨110⟩ direction and at the much lower incident energy of 28 meV. The surface temperature is 773 K. In this case the inelastic background is strongly shifted to the energy-gain side, and the agreement with calculations is again excellent. Values of $2W$ and $\hbar\omega_0$ at zero energy transfer are about 3 and 6 meV, respectively. Again, without the energy shift the data and calculations cannot be made to agree.

Figure 3 shows an energy-resolved specular scan of the scattering of a 37-meV incident beam of He on an Al(111) surface in the ⟨112⟩ direction, with the crystal temperature at 500 K.[41] The effective Debye temperature, again determined from the temperature dependence of the specular peak, is $\Theta_D = 333$ K. The solid curve shows the agreement with the calculations that is obtained using $Q_c = 1.3$ Å^{-1} and $\beta = 2.5$ Å^{-1}. The value of $2W$ is about 3 and the energy shift is somewhat more than 10 meV. Again, v_R is unimportant as the structure factor is essentially unity.

Figure 3 shows that the nature of the multiphonon background from metal surfaces is radically different from that of the alkali halides. In Figs. 1 and 2 the inelastic background formed pronounced and broad shoulders on which the specular intensity could be seen as a distinct, narrow spike. For metal surfaces the inelastic background is substantially weaker in intensity at all energies, and does not form distinct shoulders under the specular peak. This difference between insulators and metals is explained by the energy and momentum dependence of the form factor. The values of Q_c and β for Al (both choices being in agreement with typical values known for a wide range of metal surfaces[35]) imply a form factor correction as a function of energy exchange that is substantially stronger than that used for the alkali halide surfaces. These observations lead to two important conclusions: (i) the form factor of scattering by the unit cell can play a dominant role in the shape of the multiphonon background because of its strong dependence on the momentum transfer, and (ii) the strong dependence of the form factor on **k** is particularly pronounced in metals, because the potential is flat (implying small Q_c) and soft (small β), and this fact explains why the inelastic background from metals is weak and rapidly decaying as a function of energy exchange.

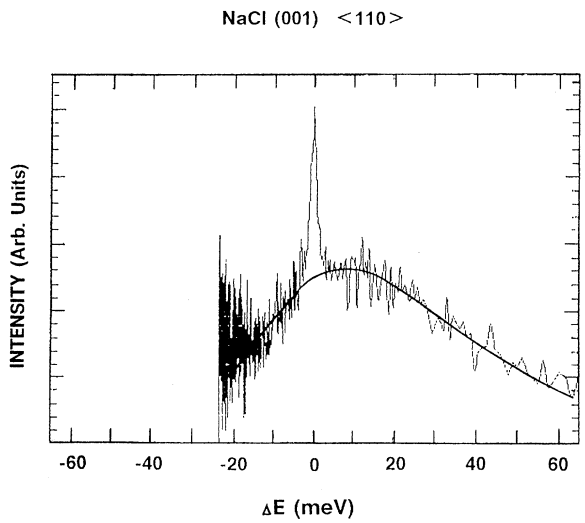

FIG. 2. Same as Fig. 1, except the scattering is in the ⟨110⟩ direction, the incident wave vector is 7.36 Å^{-1}, and the surface temperature is 773 K.

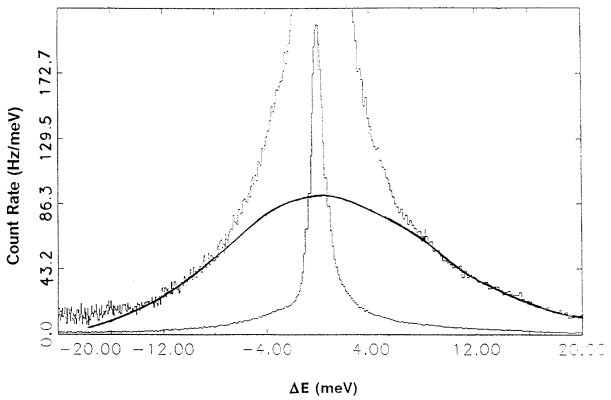

FIG. 3. Same as Fig. 1, except for an Al(111) surface in the ⟨112⟩ direction, incident wave vector of 8.37 Å^{-1}, and surface temperature of 500 K.

Figure 4 is a series of energy resolved experimental data for He scattering from a Pt(111) surface in the ⟨110⟩ direction, with $T = 160$ K and $E_i^p = 69$ meV. These are not specular scans as in the previous figures; they are scans taken with a fixed angle of 90° between incident beam and detector, with the incident angle θ_i ranging from 40° to 32°. Shown also are three different sets of theoretical calculations; the present theory, and two calculations by Celli *et al.*, one based on the Brako and Newns semiclassical limit of Eq. (53) and another using a somewhat more elaborate version of the Brako-Newns theory.[6]

This set of experimental data is interesting because it shows the importance of the structure factor in multiphonon scattering. The calculations of Celli *et al.* clearly identify a major peak structure in the data as being due to multiphonon exchange. This peak moves outward in the energy-loss direction as the angle θ_i is decreased. This peak is equally well distinguished in the present calculations, but in addition the present calculations show at $\theta_i = 37°$ and 35° the presence of a second structure, which gives rise to a substantial amount of inelastic background under the diffuse elastic peak located at $\Delta E = 0$. None of the calculations reproduces the anomalous peak appear-

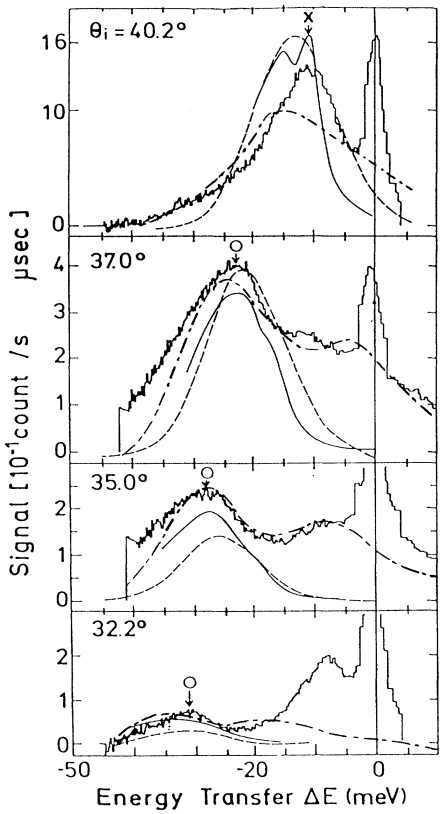

FIG. 4. The scattered intensity as a function of energy exchange for He on a Pt(111) surface in the ⟨110⟩ direction. The incident energy is 69 MeV, the surface temperature is 160 K, and the fixed angle between incident beam and detector is 90°, and four different angles of incidence are shown: (a) 40.2°, (b) 37°, (c) 35°, and (d) 32.2°. The dash-dot curve is the present calculation, while the dashed and solid curves are two different semiclassical calculations of Celli *et al.* (Ref. 6).

ing at $\Delta E \simeq -8$ meV in the $\theta_i = 32.2°$ scan.[6] This anomalous peak is critically dependent on experimental conditions and is probably due to other effects.[41] However, additional data not shown here were taken at $\theta_i = 28°$, where the anomalous peak does not appear, and the double structure evident in the present calculations at all incident angles of 35° or greater agrees well with the measurements.

Under the conditions of this experiment the structure factor differs from unity primarily because of the small mass ratio $\mu = \frac{4}{195} = 0.02$ and the low surface temperature. The structure factor has prominent peaks at the reciprocal-lattice vector positions which are at multiples of 4.52 Å^{-1} in the ⟨110⟩ direction. In addition there is a small peak halfway between at 2.26 Å^{-1} corresponding to constructive interference between scattering by alternate rows of surface atoms normal to the ⟨110⟩ direction. This second peak in $S(\mathbf{K},\omega)$ gives rise to the second multiphonon structure at smaller energy loss shown in the calculations at $\theta_i = 37°$, 35°, and 32.2°. The structure factor of the Brako-Newns semiclassical theory has only the peak centered at $\mathbf{K} = 0$, which explains why the calculations of Celli *et al.* do not exhibit the large multiphonon contribution at smaller energy transfer which appears under the diffuse elastic peak.

The Debye temperature used in the present calculations was 250 K and the sound velocity $v_R = 1234$ m/s which corresponds roughly to the Rayleigh sound velocity in Pt and is 0.65 of the value used by Celli *et al.* The parameters used for the form factor correction were $Q_c = 2$ Å^{-1} and $\beta = 10$ Å^{-1}. These parameter choices for the form factor, being quite different than expected for a metal surface, show that the form factor of the inelastic potential for such large-angle inelastic scans is very poorly known. This probably explains the rather poor overall agreement with data in the curves of Fig. 4, as opposed to the previous figures. It also underscores the importance of the potential (or form factor) in determining the shape of the inelastic background.

For these experimental conditions, the energy shifts $\hbar\omega_0$ are about 3 MeV, and $2W \simeq 0.5$ implying that a semiclassical calculation cannot be expected to give reliable results. Figure 5 shows the evolution as a function of surface temperature of the present calculations for the experimental conditions of the $\theta_i = 37°$ curve of Fig. 4. Unfortunately, there are as yet no data at higher temperatures for comparison. As the structure factor $S(\mathbf{K},\omega)$ approaches a constant at higher temperatures, the scattering intensity increases overall and gradually forms a Gaussian shape [modulated by the density of states factor in Eq. (10) peaked at an energy loss of about 15 meV]. The true semiclassical behavior of Eq. (56) is not achieved in this instance until the temperature is greater than 1200 K.

IX. CONCLUSIONS

We have presented here a treatment of inelastic scattering which is capable of providing straightforward ways of calculating the elastic, single-quantum, and the multiquantum components of the scattered intensity.

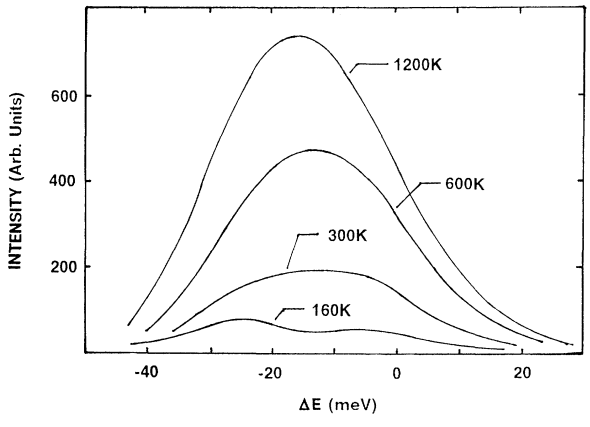

FIG. 5. Scattered intensity as a function of surface temperature for the Pt(111) surface of Fig. 4 and incident angle of 37°. Shown are five different temperatures varying from the value $T = 160$ K of Fig. 4 to $T = 1200$ K.

The motion of the particle and the surface are treated quantum mechanically, and the transition to the correspondence limit of large numbers of quanta and to the semiclassical limit for particle motion are straightforward. The treatment is based on one major approximation, that the basic elements of the surface unit cell, which can be chosen in many different ways, remain rigid while undergoing vibrational displacements. This model should work well for multiquantum processes involving the exchange of low-energy, long-wavelength phonons. A number of calculations show excellent agreement with the multiphonon inelastic background observed in He-scattering experiments. This theoretical approach shows the limits to which information on surface vibrational properties can be obtained from analysis of an experiment, without extensive knowledge of the specific and detailed nature of the He-surface interaction potential.

The treatment of the single-quantum scattering limit shows clearly the extent to which the phonon spectral density can be measured in a given experiment. For large surface unit cells, such as for reconstructed surfaces, a scattering experiment typically measures a complicated sum of surface-particle spectral densities weighted by scattering amplitudes. In the case of vicinal stepped surfaces, the greatly different nature of the scattering amplitude from the step terraces as opposed to that of the edge atoms, allows the possibility of selectively sampling the spectral density of edges or the terraces.

The treatment of the multiphonon scattering processes which forms the bulk of this work, shows the readily anticipated results such as the importance of the multiphonon intensity in identifying inelastic background in experimental data; it gives the average number of quanta exchanged in a collision, and shows the passage from quantum-mechanical to various stages of the classical limit. However, the multiphonon background is very strongly dependent on the nature of the interaction potential between incident probe and surface, and can be used to determine the form factor (modulus of the scattering amplitude) for inelastic scattering. The form factor in the present theory is the same for both single-phonon and multiphonon processes, but in single-phonon scattering the form factor always appears as a product with the phonon spectral density. Since the phonon spectral density may be imperfectly known, an experimental measurement of only the single-phonon intensity cannot separate it unambiguously from the form factor. However, the multiphonon inelastic intensity depends much more weakly on the detailed nature of the phonon spectral density, and thus allows a ready determination of the form factor for the potential. Thus a careful examination of the single-phonon peak intensities, together with measurements of the multiphonon background can be used to obtain independently the momentum and energy dependence of the scattering amplitude of the interaction potential and the phonon spectral density of the surface-phonon modes.

The treatment of multiphonon scattering allows passage to the semiclassical limit at several different levels. We find a semiclassical limit in which the coherent multiphonon background can be expressed as the product of a form factor depending on the interaction potential, a Debye-Waller factor for thermal attenuation, a structure factor arising from the periodic nature of the surface, and an energy exchange factor. The structure factor approaches unity in the extreme semiclassical limit but in the quantum regime is peaked at momentum values corresponding to the two-dimensional surface diffraction peak positions, and for complicated surface unit cells can have additional structure between the diffraction peaks.

The energy exchange function becomes a Gaussian function of the total energy exchanged between probe and surface with a shift $\hbar\omega_0$ in the direction of energy gain by the surface. The value of ω_0 depends on incident and scattered conditions, but is completely specified. However, we find that the transition to the classical limit occurs only for $2W > 6$, where $2W$ is the exponent of the Debye-Waller factor and is roughly equal to the average number of real or virtual phonons exchanged in the collision. This condition is usually not satisfied for He scattering under typical conditions involving thermal energies. The fact that the structure factor approaches a constant in the high-energy semiclassical limit implies that the interaction of the probe is constrained to a small region of coherence on the surface and in the limit involves only one surface atom. This means essentially that the major difference between scattering from an ordered surface, or from defects or disordered surfaces, arises in the nature of the scattering form factor of the interaction potential. This behavior of the structure factor is quite different from that found in previous completely semiclassical treatments using continuum models for the surface.[6,7] There it was found that the structure factor was a Gaussian function of the square of the parallel momentum exchange, modulated by an envelope in $1/T$.

We have tested this theory by comparison with a number of different experiments measuring the multiphonon background in the surface scattering of He, and very good agreement was obtained. The temperature and energy dependence of He scattered in the specular direction by a NaCl(001) surface agrees well with calculations based on a Debye model phonon spectrum, in each of the two different major crystal symmetry directions. Similar specular scan experiments for He scattering from an Al(111) surface also agree well with the calculations. The shape of the inelastic background is quite different for the alkali halide and metal surfaces. For NaCl the elastic intensity appeared as a distinct narrow peak sitting on the broad shoulders of a well-defined background, while for the Al surface the multiphonon background appeared as tails leading away from the elastic peak. The difference is readily explained by the nature of the form factor of the interaction potential; as compared to the alkali halide, the weakly inelastically scattering metal surface has a softer repulsive potential and is much smoother and flatter. The comparison shows the strong dependence of the multiphonon background on the interaction potential and the power of this method for extracting such information.

A comparison with experiment was made for the scattering of He by a Pt(111) surface in the $\langle 110 \rangle$ direction at relatively low surface temperature. Measurements were made of background intensity versus energy ex-

change in several nonspecular scattering directions, and a comparison with other calculations was possible. It is found that the conditions are sufficiently quantum mechanical that the structure factor deviates substantially from its semiclassical value of unity, and this structure is observed in the experiment.

We have found that the multiphonon inelastic background in a surface-scattering experiment is strongly dependent on the nature of the interaction potential, but rather weakly dependent on the details of the phonon spectrum and hence can be calculated using simple models. In addition to its usefulness in subtracting off background, the comparison with experiment of calculated multiphonon intensities determines the form factor, and thus provides useful information on the interaction potential.

ACKNOWLEDGMENTS

The author would like to thank J. Skofronick, V. Celli, D. Himes, J. P. Toennies, A. Lock, and J. Black for helpful and stimulating discussions. Support by the Alexander von Humboldt Foundation is gratefully acknowledged. We would like to thank A. Lock, M. Gosler, J. Skofronick, and J. P. Toennies for making the data available before publication.

---

*Permanent address.

[1]V. Bortolani and A. C. Levi, Riv. Nuovo Cimento **9**, 1 (1986); J. P. Toennies, J. Vac. Sci. Technol. A **2**, 1055 (1984).

[2]C. S. Jayanthi, H. Bilz, W. Kress, and G. Benedek, Phys. Rev. Lett. **52**, 429 (1984).

[3]*Handbook on Synchrotron Radiation,* edited by D. E. Monchton and G. S. Brown (North-Holland, Amsterdam, 1987), Vol. 3.

[4]J. B. Pendry, *Low-Energy Electron Diffraction* (Academic, New York, 1974); M. A. Van Hove and S. Y. Tong, *Surface Crystallography by LEED* (Springer-Verlag, Berlin, 1979).

[5]G. Benedek and L. Miglio, in *Helium Atom Scattering: A Gentle and Sensitive Tool in Surface Science,* edited by E. Hulpke (Springer-Verlag, Heidelberg, 1990); B. Feuerbacher and D. Neuhaus, *ibid.*

[6]V. Celli, D. Himes, P. Tran, J. P. Toennies, Ch. Wöll, and G. Zhang (unpublished).

[7]R. Brako and D. M. Newns, Phys. Rev. Lett. **48**, 1859 (1982); J. Phys. C **14**, 3605 (1981); Surf. Sci. **117**, 422 (1982); R. Brako, *ibid.* **123**, 439 (1982).

[8]H. D. Meyer and R. D. Levine, Chem. Phys. **85**, 189 (1984).

[9]David A. Micha, J. Chem. Phys. **74**, 2054 (1981).

[10]W. Brenig, Z. Phys. B **36**, 81 (1979); J. Böheim and W. Brenig, *ibid.* **41**, 243 (1981).

[11]D. Kumamoto and R. Silbey, J. Chem. Phys. **75**, 5164 (1981).

[12]J. Lorenzen and L. M. Raff, J. Chem. Phys. **74**, 3929 (1981); P. M. Argrawal and L. M. Raff, *ibid.*, **77**, 3946 (1982); M. Jezercak, P. M. Agrawal, C. Smith, and L. M. Raff, *ibid.* **88**, 1264 (1988).

[13]B. Jackson, J. Chem. Phys. **88**, 1383 (1988); **92**, 1458 (1990).

[14]L. Van Hove, Phys. Rev. **95**, 249 (1954).

[15]R. Glauber, Phys. Rev. **87**, 189 (1952); **98**, 1692 (1955).

[16]R. Weinstock, Phys. Rev. **65**, 1 (1944).

[17]A. Sjölander, Ark. Fys. **14**, 315 (1959).

[18]A. A. Maradudin, E. W. Montroll, and G. H. Weiss, in *Solid State Physics: Theory of Lattice Dynamics in the Harmonic Approximation* (Academic, New York, 1963), Suppl. 3.

[19]R. Manson and V. Celli, Surf. Sci. **24**, 495 (1971).

[20]G. Armand and J. R. Manson, Phys. Rev. Lett. **53**, 1112 (1985); C. S. Jayanthi, G. Armand, and J. R. Manson, Surf. Sci. **154**, L247 (1985); G. Armand and J. R. Manson, J. Phys. (Paris) **47**, 1357 (1986).

[21]V. Bortolani, A. Franchini, and G. Santoro, in *Dynamical Phenomena at Surfaces, Interfaces, and Superlattices,* edited by F. Nizzoli, K. H. Rieder, and R. F. Willis (Springer-Verlag, Berlin, 1985), p. 92.

[22]V. Celli, in *Dynamical Properties of Solids,* edited by G. K. Horton and A. A. Maradudin (Elsevier, New York, 1990).

[23]A. Lock and J. Black (unpublished).

[24]A. Lahee, J. R. Manson, J. P. Toennies, and Ch. Wöll, Phys. Lett. **57**, 471 (1986).

[25]B. J. Hinch and J. P. Toennies, Phys. Rev. B **42**, 1209 (1990).

[26]J. Perreau and J. Lapujoulade, Surf. Sci. **119**, L292 (1982); **122**, 341 (1982).

[27]C. W. Skorupka and J. R. Manson, Phys. Rev. B **41**, 9783 (1990).

[28]R. E. Allen, G. P. Alldredge, and F. W. de Wette, Phys. Rev. B **4**, 1648 (1971); **4**, 1661 (1971); **4**, 1682 (1971).

[29]G. Benedek, Phys. Status Solidi B **58**, 661 (1973); Surf. Sci. **61**, 603 (1976); G. Armand, Phys. Rev. B **14**, 2218 (1976).

[30]E. Hulpke, Surf. Sci. **52**, 615 (1975).

[31]U. Gerlach-Meyer and E. Hulpke, Chem. Phys. **22**, 325 (1977).

[32]J. Beebe, J. Phys. C **7**, L359 (1971).

[33]R. I. Masel, Surf. Sci. **77**, L179 (1978).

[34]J. R. Manson and G. Armand, Surf. Sci. **184**, 511 (1987).

[35]V. Celli, G. Benedek, U. Harten, J. P. Toennies, R. B. Doak, and V. Bortolani, Surf. Sci. **143**, L376 (1984).

[36]F. O. Goodman and H. Y. Wachman, *Dynamics of Gas—Surface Scattering* (Academic, New York, 1976).

[37]G. Chern, J. G. Skofronick, W. P. Brug, and S. A. Safron, Phys. Rev. B **39**, 12 828 (1989).

[38]W. P. Brug, G. Chern, J. Duan, S. A. Safron, and J. G. Skofronick, J. Vac. Sci. Technol. A **8**, 2632 (1990).

[39]S. A. Safron, W. P. Brug, G. Chern, J. Duan, J. G. Skofronick, and J. R. Manson, J. Vac. Sci. Technol. A **8**, 2627 (1990).

[40]G. Chern, G. Bishop, J. Duan, J. G. Skofronick, W. P. Brug, S. A. Safron, and J. R. Manson (unpublished).

[41]G. Zhang (private communication).